

Self-similar tendency of metabolic networks: as in the case of bow-tie structure

Jing Zhao^{1,2,4}, Hong Yu², Jian-Hua Luo¹, Zhi-Wei Cao^{2§}, Yi-Xue Li^{2,3,1§}

¹Department of Biomedical Engineering, Shanghai Jiao Tong University, Shanghai 200240, China

²Shanghai Center for Bioinformation and Technology, Shanghai 200235, China

³Shanghai Institutes for Biological Sciences, Chinese Academy of Sciences, Shanghai 200031, China

⁴Department of mathematics, Logistical Engineering University, Chongqing 400016, China

[§]Corresponding author

Email addresses:

JZ: zjane_cn@sjtu.edu.cn

HY: yuhong@scbit.org

JHL: jhluo@sjtu.edu.cn

ZWC[§]: zwcao@scbit.org

YXL[§]: yxli@sibs.ac.cn

Abstract

Background

The exploration of the structural topology and the organizing principles of genome-based large-scale metabolic networks is essential for studying possible relations between structure and functionality of metabolic networks. Topological analysis of graph models has often been applied to study the structural characteristics of complex metabolic networks.

Results

In this work, metabolic networks of 75 organisms were investigated from a topological point of view. Network decomposition of three microbes (*Escherichia coli*, *Aeropyrum pernix* and *Saccharomyces cerevisiae*) shows that almost all of the sub-networks are functionally related modules exhibiting a similar bow-tie topological pattern as that of the global metabolic networks. Moreover, these small bow-ties are hierarchically nested into larger ones and collectively integrated into a large metabolic network, which is not observed in the random shuffled network. Such a bow-tie pattern appears to be present in certain chemically isolated functional modules and spatially separated modules including carbohydrate metabolism, cytosol and mitochondrion respectively.

Conclusions

The bow-tie pattern is present at different levels and scales, and in different chemical and spatial modules of metabolic networks, which is likely the result of the evolutionary process rather than a random accident. Identification and analysis of

such a pattern is helpful for understanding the design principles and facilitate the modelling of metabolic networks.

Background

Cellular metabolism is an essential process for the maintenance of life and metabolic networks have been extensively studied [1-5]. Although a large variety of metabolic reactions can be found in different organisms, metabolic networks are highly conserved across them. It remains to be a highly interested and challenging problem to understand the architectural characteristics and “design” principles of the metabolic networks in relation to their function. A remarkable finding is that metabolic networks, as well as other real-world complex networks, have topologies that differ markedly to those found in simple randomly connected networks [6], which suggests that their non-random structures could imply significant organizing principles of metabolic networks.

One of the main characteristics of metabolic networks is that they appear to be organized in a hierarchical-modularity manner. Efforts have been directed towards the recognition of such a feature in metabolic networks. By applying the power-law scaling of the clustering coefficient as an indicator, Ravasz et al. have suggested that metabolic networks may be organized as many small compacted modules connected in a hierarchical manner [7, 8]. On the other hand, Trusina et al. have investigated the hierarchical topology of networks based on the notion of a hierarchical path [9]. Recently, Song et al. have adopted a box-counting algorithm from a fractal geometry method to distinguish hierarchical networks. They have found that many complex networks observed in nature, including metabolic networks, could be self-similar in

the sense of degree distribution of nodes [10], although the functional significance of those boxes remains to be determined [11]. These works provide useful hints about some of the “design” principles of metabolic networks, and they suggest that a further investigation is warranted for probing the correlation between local structural components and global topological functionality in these networks [12].

Several algorithms have been developed to detect modular components in metabolic networks. These include the method of topological overlap matrix [7], the node degree method [13], simulated annealing [14], the edge betweenness centrality method [15], and hierarchical decomposition based on dependency [16]. In addition, it has been discovered, that the global metabolic network is organized in the form of a bow-tie [17]. On the basis of such a bow-tie topology, Ma and Zeng have proposed a decomposing algorithm based on the shortest path combined with “majority rule” [18]. Furthermore, Newman and Girvan have come up with a modularity parameter as a quantitative criterion to evaluate the decomposing quality of a network, where a good decomposition will result in relatively isolated modules with many within-module links and as few as possible between-module links [19]. These methodologies are useful for conducting metabolic network decomposition studies.

In this work, 75 metabolic networks were constructed from organisms including 8 eukaryote, 56 bacteria and 11 archaea. By applying the decomposing method similar to [18], the topological features of various graph models were studied at different levels, sub-cellular localizations, and biochemical pathways in the form of bow-tie. To mine the inherent topology of metabolic networks, the features from *E.coli* network were then compared with those of a properly randomised version that

preserves the linkage degree of each node and the total number of directed and bi-directed arcs [20].

Results/Discussion

Decomposing the metabolic networks

The metabolic networks of three microbes (*Escherichia coli*, *Aeropyrum pernix* and *Saccharomyces cerevisiae iND750*) were decomposed. Only the results of the *E.coli* network are presented in this paper for illustration. The other two networks displays similar features as the *E.coli* network and the relevant analysis results are provided in the supplementary material (part I and II).

The metabolic network of *E. coli* K-12 MG1655 consists of 934 nodes and 1437 arcs. The largest connected part of this network embraces 575 nodes and its topology exhibits a bow-tie architecture. A typical bow-tie consists of four parts: giant strong component (GSC), substrate subset (S), product subset (P) and isolated subset (IS). The GSC is the biggest of all strongly connected components, in which any pair of nodes has a directed path between them. To further decrease the complexity, the GSC part is reduced to a Core through the method of [17].

The hierarchical clustering tree for the Core of the GSC, obtained by our decomposition algorithm, is shown in Figure 1. According to the modularity parameter from Newman and Girvan [19], 12 clusters of the Core appeared as shown in Figure 2. Figure 3 illustrates the decomposition of the whole metabolic network.

To examine whether there is a functional relevance for each module, the reactions of each module were mapped to KEGG pathway [22, 23] (<http://www.genome.jp/kegg/pathway.html>). A cartographic representation [14] of the metabolic network is shown in Figure 4(A), in which each node corresponds to a cluster in Figure 3. The colours in Figure 4(A) represent different categories of metabolism while the coloured areas indicate the percentage of respective metabolism within the module. This illustrates that most modules generated by our algorithm are dominated by one major category of metabolism (more than 50%). For instance, the reactions in the 3rd module are mainly carbohydrate metabolisms that include a complete TCA cycle, as shown in Figure 4(B). Only two modules (module 1 and 5) cannot simply be associated with a major colour. When examining the nodes in module 1 and 5 we found that there are heavily overlapping compounds both by carbohydrate and amino acid metabolism. It is difficult to assign these metabolites to a single module because they are playing dual and even multiple roles in several metabolism processes. For example, pyruvate in the 1st module is a key metabolite that connects the metabolism of carbohydrates, amino acids and the energy metabolism. Secondly, different categories of metabolisms can actually be grouped together through close topological linkage, as shown in Figure 3. This grouping from topology may provide useful hints in the relationship between them, as well as to the functional significance of those unknown reactions.

Self-similarity of metabolic networks in the case of bow-tie structure

To further investigate the macroscopic structure of each sub-network in Figure 3, the node distributions in the bow-tie structure of the sub-networks were listed in Table 1. It can be seen that almost all of the twelve sub-networks have formed bow-tie structures, similar to the global network. The only exception is the 6th module, which

doesn't have the P part. It could be treated as a kind of degraded bow-tie, because such cases have been reported in natural structures indicating the sub-structures do not always display perfect similarity to that of the global structure [24, 25].

A coarse-grained graph is given in Figure 5 to illustrate the connections between the GSC parts of the sub-networks. Each node in Figure 5 corresponds to a cluster in Figure 3, while two nodes in Figure 5 are defined as being connected if and only if the constituent nodes in corresponding GSC parts are linked. Such connecting topology is different from that in Figure 4, in which the arcs correspond to the links between the sub-networks.

It is thus noted from the definition of strongly connected graphs that, if some nodes in Figure 5 can be combined into a strongly connected sub-graph, the merger of the corresponding sub-networks may form a bigger bow-tie whose GSC is the union of the individual GSC parts [26]. For example, the unions of clusters, such as {1,2,3}, {1,3,4}, {5,8,10,11,12}, and the union of all the twelve clusters have bow-tie structures, but the following clusters {1,2}, {4,9,10}, {10,11,12} can't form strongly connected sub-graphs, thus are not bow-tie. In this way, different sub-networks of bow-tie structures can be combined to form bigger bow-ties at higher level.

The combination of different bow-ties was also compared with the global bow-tie from proportional scale. One hundred and fifty bow-ties were hierarchically generated by random combinations of a number of basic bow-ties from the coarse-grained graph in Figure 5. Their node distributions of the four parts (GSC, S, P, and IS) were listed in Table S3 of the supplementary material. The percentage discrepancies of the four

parts to those of the global one were also summarized in Table S3. Interestingly, the node distribution of the nested bow-ties is approximately consistent with that of the global network with an average absolute error of 0.0854, which means each smaller bow-tie can be considered as a miniature of the global one.

In this sense, metabolic networks seem to be designed in such a way that many similar small structural units, which are hierarchically nested and reoccur at different scales and levels, are coupled level-by-level into a larger network. Therefore, metabolic networks appear approximately self-similar in terms of the repetition of a unit pattern at different levels and different sizes, just like the map of a coastline that is not identical but statistically matches the average proportion when magnified [24, 25].

Comparison between the *E.coli* network and a random connected network

To examine whether the nested bow-ties are intrinsic to metabolic networks, a random model network was constructed by reshuffling the links of the *E.coli* metabolic network [20]. The in- and out-degree of each node, as well as the total number of directed and bi-directed arcs of the *E.coli* metabolic network, are preserved in this “artificial” model network. Topological analysis revealed that the global structure of this random network still preserves bow-tie topology, but the average clustering coefficient does not follow the power law, as Figure 6 shows. According to the theory of Ravasz et al. [7, 8], this random network is not a hierarchically modular network, which is different from the real metabolic network. This result indicates that the self-similarity of bow-tie structures is an intrinsic and significant feature of metabolic networks, rather than a random phenomenon.

Self-similar bow-tie topology from a chemical and spatial viewpoint

Assuming that self-similarity is common to metabolic networks, the bow-tie may be observed from various systems such as cellular organelles and metabolic pathways of fundamental bio-molecules. Reactions of the three basic metabolisms, carbohydrate metabolism, lipid metabolism, and amino acid metabolism, were retrieved from the database of [27] for 75 organisms (Eukaryote: 8; Bacteria: 56; Archaea: 11). Our analysis shows that all the reactions in carbohydrate metabolism have framed a bow-tie structure for all the examined organisms, as being provided by part IV of the supplementary material. But neither the lipid reactions nor the amino acid reactions can build a bow-tie. This could be caused by the different roles they play. Carbohydrate metabolism breaks down sugars and the energy can be directly utilized by other processes of life in an organism. In contrast, the products of lipid metabolism and amino acid metabolism are intermediate products and need to be further transformed to carbohydrates for energy production. In this sense, carbohydrate metabolism is a relatively independent metabolic process, compared to lipid metabolism and amino acid metabolism.

Similar analysis was done to the reactions of the *Saccharomyces cerevisiae* iND750 [28] according to sub-cellular localisations. Three cellular compartments, cytosol, mitochondrion, and peroxisome, were studied which include relatively more metabolites. It was found that the sub-networks of cytosol reactions and mitochondrion reactions could exhibit the bow-tie patterns as shown in Table 2. It is known that mitochondrion is functionally relatively independent organelle, while the majority of metabolic reactions take place in cytosol. That the peroxisome reactions do not form a bow-tie could be caused by the scarcity of reaction information of

peroxisome. However, with the development of genomics, proteomics and metabonomics, and the accumulation of sub-cellular information of more reactions, we speculate that it is possible to find bow-tie structures in more organelles.

In brief, bow-tie pattern is also present in elementary metabolism such as carbohydrates, and in cellular compartments of mitochondria and cytosol. These results indicate that the self-similarity feature of bow-tie patterns is common to metabolic networks. At the same time, the complete bow-tie patterns in mitochondria and carbohydrates pathways could also imply some independent functional clues.

Significance of self-similarity in the form of bow-tie structure

In the long evolutionary process of metabolism networks and their components, the structure of self-similar modularity could contribute significantly to the function of metabolic networks. To begin with, self-similarity often signifies the efficiency of a system, as in the case of the Lego toy system [29]. In our work, the recurrence of bow-tie structures suggests that bow-tie modules may act as another kind of building block of the genome-based metabolic network during the evolutionary process, indicating that evolution might copy and reuse existing modules to give rise to ever higher forms of complexity when new function calls for it.

Another contribution would be network robustness. We studied the top twenty hub nodes with a degree of at least 10 and the linkage among them from the metabolic network of *E.coli* (Figure 7). Table 3 lists the distribution of these twenty hubs in the twelve functional modules, their total degrees and within-module degrees. It was found that most of the hubs have no immediate links between them, while have a

large within-module linkage as shown in Table 3. In other words, the densely connected hubs tend to scatter in different modules, while the unit modules are organized separately around individual hubs. Such a connection pattern of metabolic networks decreases the likelihood of cross talk between different functional modules, and may provide a certain degree of protection against attacks aimed at hubs by confining damage to separable parts.

Moreover, selection of bow-tie as a building unit seems to be a concise and smart option for constructing metabolic networks. As we know, “bow-tie” structure is characteristic of various inputs and outputs that are connected by a knot of intermediary metabolism [30, 31]. Such a structure has been reported to be present in various biological systems, such as in signal transduction systems, transcription and translation processes, and immune systems [30-34]. For instance, the glucose homeostasis is configured as a bow-tie structure, where glucose is the common carrier in the knot [30, 34]; the intercellular interactions of the immune system form bow-tie network whose knot consists of the CD4+T-cells [32]. In metabolic networks, if every substrate-product combination follows independent pathways without sharing common intermediary metabolites, the total genome would be much larger and its encoded enzymes would be vastly more complex [30]. On the other hand, the knot of the bow-tie is the most tightly connected part of the network such that multiple routes exist between any pair of nodes, possibly creating alternative pathways to meet an emergency or process new metabolites.

Conclusions

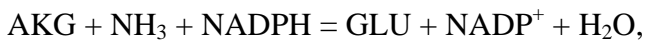
In this survey we have attempted to reveal the topological features of graph models from the view of the design principle of metabolic networks. Our results suggest that metabolic networks exhibit approximate self-similarity in the form of bow-tie structures, whereas this feature is not present in random graphs with comparable statistical weight. This finding is consistent with the conclusions from a number of studies that these structures result from universal and fundamental organizing principles for efficiency and robustness, rather than frozen accidents of evolution. It is possible that the self-similarity of metabolic networks could emerge in different patterns, while the bow-tie is only one of them. On the other hand, self-similarity may also be the result of natural selection of biological evolution, which could be conceived as a process where the same patterns and processes repeat at each stage, and are nested at multilevel [35-38]. The perspectives of this paper would provide useful hints for understanding the function and evolution of metabolic networks, as well as the modeling and simulation of complex biological systems.

Methods

Data preparation

In this study, the metabolic data were extracted from the database developed by Ma and Zeng based on the Kyoto Encyclopedia of Genes and Genomes (KEGG) [27]. In this database, the information concerning the reversible reactions was specified. In addition, some small molecules, such as adenosine triphosphate (ATP), adenosine diphosphate (ADP), nicotinamide adenine dinucleotide (NAD) and H_2O , are normally used as carriers for transferring electrons or certain functional groups and participate

in many reactions, while typically not participating in product formation. Therefore, in order to reflect biologically relevant transformations of substrates, these kinds of small molecules, as well as their connections were manually excluded from the database when no products were formed from them. It should be noted that this method of exclusion is not determined by compounds, but by the reaction. For example, glutamate (GLU) and 2-oxoglutarate (AKG) are current metabolites for transferring amino groups in many reactions, but in the following reaction:



AKG participates in producing GLU, i.e., they are primary metabolites. Hence the connections through them should be considered. A metabolic network reconstructed from this database is represented by a directed graph whose nodes correspond to metabolites and whose arcs correspond to reactions between these metabolites, in which a reversible reaction is treated as two irreversible reactions and corresponds to a bi-directed arc.

The metabolic network iND750, a fully compartmentalized genome-scale metabolic model of *Saccharomyces cerevisiae* constructed by Duarte et al. [28], was then studied. This set of data is the most complete metabolic data in the public domain that includes information on sub-cellular localization. Compartmentalization of information, which includes the localization to the cytosol, Golgi apparatus, mitochondrion, nucleus, endoplasmic reticulum, vacuole, peroxisome, or extracellular space, is given for each reaction. Reactions were assigned to the cytosol by default unless there was evidence that a metabolite was found in a particular compartment.

Referring all the reactions in iND750 to the database of [27], we manually removed the connections through current metabolites, such as H_2O , ATP, NADH, thus the reconstructed network of *S. cerevisiae* is represented as a directed graph.

Algorithm to decompose the genome-based metabolic network

Our decomposition algorithm is similar to that of [18] which is based on the bow-tie structure of metabolic networks, while a different dissimilarity index is used. In addition, since many linear branches, which consist of several reversible reactions, exist in the GSC part, removing these linear branches will lead to the Core of the GSC, which is still strongly connected [17]. Our algorithm begins with decomposing the Core part into sub-networks that are still strongly connected, or most of the nodes are strongly connected. Since the GSC part of the metabolic network includes abundant bi-directed arcs corresponding to reversible reactions [17], and that a sub-graph which consists of plentiful bi-directed arcs is more likely to be strongly connected, the nodes in the Core part should be distributed into clusters so that most links within the same cluster are bi-directed arcs, while most links between different clusters are directed arcs. A simple example is given in Figure 8 (a). If this simple strongly connected graph could be broken down into two parts $\{2, 3, 4\}$ and $\{1, 7, 6, 5\}$ by a certain algorithm, it would be decomposed into two strongly connected components. The dissimilarity index $D(i, j)$ between vertex i and j , which quantitatively measures the extent that two vertices are likely to appear in the same sub-network, can be defined as the corrected Euclidean-like dissimilarity [39],

$$D(i, j) = \sqrt{\sum_{\substack{k=1 \\ k \neq i, j}}^N [(d_{ik} - d_{jk})^2 + (d_{ki} - d_{kj})^2] + (d_{ij} - d_{ji})^2}. \quad (1)$$

where d_{ij} is the distance from node i to node j , which is the number of arcs in the shortest directed path from i to j (in general, $d_{ij} \neq d_{ji}$). The distance between all node pairs can be computed by Floyd algorithm [26].

Having obtained the dissimilarity indexes, Ward's clustering, a hierarchically agglomerative clustering method, is used to decompose the network [40]. This algorithm produces a hierarchical clustering tree, or a dendrogram, for the network. Finally, the decomposition of the Core part can be expanded to the global network by using the “majority rule” proposed by Ma and Zeng [18]. The algorithm steps are presented as follows:

1. Remove all the linear branches of the GSC part and get the Core.
2. Decompose the Core of the GSC by Ward's clustering based on the dissimilarity index of equation (1) and get its hierarchical clustering tree.
3. Cut the hierarchical clustering tree into m clusters so that the value of modularity parameter is the largest [19].
4. Expand the clusters of the Core to the whole metabolic network by the “majority rule”, i.e., the nodes that are directly connected to nodes in GSC are placed in the subset to which most of their neighbours in GSC belong; the other nodes are classified into corresponding subsets to which most of their neighbours belong.

The dendrogram for the network in Figure 8(a) obtained by this algorithm is shown in Figure 8(b), suggesting that this method can decompose the strongly connected graph, as we required.

Algorithm to generate the model network

A method similar to that of Maslov and Sneppen [20] was used to generate a model network. This algorithm randomly reshuffles the links of the original network, while

preserving the in- and out-degree of each node, as well as the total number of directed and bi-directed arcs. It is presented as follows:

1. Partition all the arcs of the original network into directed arcs and bi-directed arcs.
2. Reshuffle the bi-directed arcs: Randomly select a pair of bi-directed arcs $A \leftrightarrow B$ and $C \leftrightarrow D$. Rewire the two bi-directed arcs to get links $A \leftrightarrow C$ and $B \leftrightarrow D$, if there are neither directed nor bi-directed arcs between the pair $A-C$ and $B-D$ respectively. Otherwise, abandon this pair and chose another pair of bi-directed arcs. The last restriction prevents the appearance of multiple arcs between the same pair of nodes. In addition, the network should always remain connected during the rewiring process.
3. Reshuffle the directed arcs: Randomly select a pair of directed arcs $A \rightarrow B$ and $C \rightarrow D$. Rewire the two directed arcs to get links $A \rightarrow D$ and $C \rightarrow B$. As in step 2, during the rewiring process, multiple links are prohibited, and the network should always remain connected.

Repeating step 2 and step 3 many times will generate a randomly connected counterpart of the original network.

Authors' contributions

JZ conceived of the study, designed the analysis, implemented the analysis and prepared the manuscript. HY implemented the analysis. JHL managed the project. ZWC and YXL helped JZ to design the analysis, provided guidance, coordinated and participated in the biological and theoretical analyses, and revised the manuscript. All authors read and approved the final manuscript.

Acknowledgements

This work is supported by National Basic Research Programs of China (No. 2003CB715901, 2004CB720103, 2004BA711A21), Science and Technology Committee of Shanghai (04QMX1450, 04DZ14005). We thank Dr. H.W. Ma and A.P. Zeng for providing us with their metabolic networks' database. We also thank Dr. Y. Z. Chen for critical reading of this paper.

References

1. Stelling J, Klamt S, Bettenbrock K, Schuster S, Gilles ED: **Metabolic network structure determines key aspects of functionality and regulation.** *Nature* 2002, **420**: 190-193.
2. Wagner A, Fell DA: **The small world inside large metabolic networks.** *Proc. R. Soc. Lond. B* 2001, **268**:1803–1810.
3. Jeong H, Tombor B, Albert R, Oltvai Z N, Barabasi A L: **The large-scale organization of metabolic networks.** *Nature* 2000, **407**:651–654.
4. Tanaka: **Scale-rich metabolic networks.** *Physical Review Letters* 2005, **94**: 168101.
5. Arita M: **The metabolic world of Escherichia coli is not small.** *PNAS* 2004, **101**: 1543–1547.
6. Erdos P, Renyi A: **On the evolution of random graphs.** *Publ. Math. Inst. Hung. Acad. Sci.* 1960, **5**:17-61.

7. Ravasz E, Somera A L, Mongru D A, Oltvai Z N, Barabasi A L: **Hierarchical organization of modularity in metabolic networks.** *Science* 2002, **297**: 1551-1555.
8. Ravasz E, Barabasi A L: **Hierarchical organization in complex networks.** *Phys. Rev. E* 2002, **67**: 026122.
9. Trusina A, Maslov S, Minnhagen P, Sneppen K: **Hierarchy measures in complex networks.** *Phys. Re. Lett.* 2004, **92**:178702.
10. Song C, Havlin S, Makse H A: **Self-similarity of complex networks.** *Nature* 2005, **433**:392-395.
11. Strogatz S H: **Romanesque networks.** *Nature* 2005, **433**:365-366.
12. Monk N A M: **Unravelling Nature's networks.** *Biochem. Soc. Trans* 2003, **31**:1457-1461.
13. Schuster S, Pfeiffer T, Moldenhauer F, Koch I Dandekar T: **Exploring the pathway structure of metabolism: decomposition into subnetworks and application to *Mycoplasma pneumoniae*.** *Bioinformatics* 2002,**18**:351-361.
14. Guimera R, Amaral L A N: **Functional cartography of complex metabolic networks.** *Nature* 2005, **433**: 895-900.
15. Holme P, Huss M, Jeong H: **Subnetwork hierarchies of biochemical pathways.** *Bioinformatics* 2003, **19**:532-538.
16. Gagneur J, Jackson D B, Casari G: **Hierarchical analysis of dependency in metabolic networks.** *Bioinformatics* 2003, **19**: 1027-1034.
17. Ma H W, Zeng A P: **The connectivity structure, giant strong component and centrality of metabolic networks.** *Bioinformatics* 2003, **19**: 1423-1430.
18. Ma H W, Zhao X M, Yuan Y J, Zeng A P: **Decomposition of metabolic network into functional modules based on the global connectivity structure of reaction graph.** *Bioinformatics* 2004, **20**:1870-1876.
19. Newman M. E. J., Girvan M.: **Finding and evaluating community structure in networks.** *Phys. Rev. E* 2004, **69**:026113.
20. Maslov S, Sneppen K: **Specificity and stability in topology of protein networks.** *Science* 2002, **296**: 910-913.
21. Batagelj V, Mrvar A: **Pajek-program for large network analysis.** *Connections* 1998, **21**:47-57.
22. Goto S, Nishioka T, Kanehisa M: **LIGAND: chemical database for enzyme reactions.** *Nucleic Acids Research* 2000, **28**:380-382.

23. Goto S, Okuno Y, Hattori M, Nishioka T, Kanehisa M: **LIGAND: database of chemical compounds and reactions in biological pathways.** *Nucleic Acids Res* 2002, **30**:402–404.

24. Mandelbrot B: *The fractal geometry of nature.* New York, W. H. Freeman 1983.

25. Komulainen T: **Self-Similarity and Power Laws.** In: *Complex Systems - Science on the Edge of Chaos.* Edited by Hyötyniemi H. Helsinki University of Technology, Control Engineering Laboratory, Report 145, 2004, 109-120.

26. Bondy J A, Murty U S R: *Graph theory with applications.* London, Macmillan 1976.

27. Ma H W, Zeng A P: **Reconstruction of metabolic networks from genome data and analysis of their global structure for various organisms.** *Bioinformatics* 2003, **19**:270–277.

28. Duarte N C, Herrgard M J, Palsson B: **Reconstruction and validation of *Saccharomyces cerevisiae* IND750, a fully compartmentalized genome-scale metabolic model.** *Genome Research* 2004, **14**:1298-1309.

29. Csete M, Doyle J: **Reverse Engineering of Biological Complexity.** *Science* 2002, **295**: 1664-1669

30. Csete M, Doyle J: **Bow-ties, metabolism and disease.** *Trends in Biotechnology* 2004, **22**: 446-450.

31. Kitano H: **Biological robustness.** *Nature Reviews Genetic* 2004, **5**:826-837.

32. Kitano H, Oda K, **Robustness trade-offs and host-microbial symbiosis in the immune system.** *Molecular Systems Biology* 2006, **2**: msb4100039-E1-msb4100039-E10.

33. Marhla M, Perca M, Schuster S, **Selective regulation of cellular processes via protein cascades acting as band-pass filters for time-limited oscillations.** *FEBS Letters* 2005, **579**: 5461–5465.

34. Kitano H, Oda K, Kimura T, Matsuoka Y, Csete M, Doyle J, Muramatsu M: **Metabolic Syndrome and Robustness Tradeoffs.** *Diabetes* 2004, **53**:S6-S15.

35. West G B, Brown J H, Enquist B J: **A general model for the origin of allometric scaling laws in biology.** *Science* 1997, **276**:122-126.

36. West G B, Brown J H, Enquist B J: **The fourth dimension of life: fractal geometry and allometric scaling of organisms.** *Science* 1999, **284**:1677-1679

37. Rani M: **Dynamics of protein evolution.** *J. Biosci.* 1998, **23**:47-51.

38. Werner C., Rasskin-Gutman D: *Modularity: Understanding the Development and Evolution of Natural Complex Systems.* Cambridge, MIT Press 2005 .

39. Batagelj V, Mrvar A, Ferligoj A, Doreian P: **Generalized blockmodeling with Pajek.** *Metodoloski Zvezki* 2004, **1**: 455-467.
40. Ward J: **Hierarchical grouping to optimize an objective function.** *J. Amer. Statist. Assoc.* 1963, **58**:236-244.

Figures

Figure 1

The hierarchical clustering tree for the Core of the GSC for *E.coli* network

Figure 2

Decomposition of the Core for the GSC of *E.coli* metabolic network. This graph is drawn with the graph analysis software Pajek [21], in which different clusters are shown in different colours.

Figure 3

Decomposition of the *E.coli* metabolic network. Different clusters are shown in different colours.

Figure 4

(A) Cartographic representation of the metabolic network for *E.coli*. Each circle represents a module and is coloured according to the KEGG pathway classification of the reactions belonging to it, while the arcs reflect the connection between clusters. The area of each colour in one circle is proportional to the number of reactions that belong to the corresponding metabolism. The width of

an arc is proportional to the number of reactions between the two corresponding modules. For simplicity, bi-directed arcs are presented by grey edges.

(B) Bio-reactions in the 3rd module. Each node represents a metabolite and is coloured according to the class of metabolism it participates in. This module contains TCA recycle, in which the reactions are highlighted by red arrows.

Figure 5

The connections among the GSC parts of the twelve bow-tie like functional modules. The width of an arc is proportional to the number of links between the GSC parts of the two corresponding modules. For simplicity, bi-directed arcs are presented by grey edges.

Figure 6

The relationship of clustering coefficient with the node's degree. $C(k)$ is defined as the average clustering coefficient of all nodes with k links. That $C(k)$ obeys the power law is an indication of a network's hierarchical modularity feature, while $C(k)$ is independent of k in non-hierarchical networks [7, 8].

(A) $C(k)$ obeys the power law for the metabolic network of *E.coli*

(B) $C(k)$ is independent of k for the model network, which has the same number of nodes, arcs and degree distribution with the *E.coli* metabolic network.

Figure 7

Distribution and links of hubs in the metabolic network of *E.coli*. Nodes of different colours belong to different functional modules in Figure 3.

Figure 8

A simple strongly connected graph and the dendrogram obtained by our algorithm.

(A) A simple strongly connected graph

(B) Dendrogram

Tables

Table 1 Node distributions in the global structure of sub-networks obtained from the decomposition for *E.coli* network

* D: degraded bow-tie

Cluster	Total nodes	GSC		S		P		IS		Bow-tie
		nodes	percent	nodes	percent	nodes	percent	nodes	percent	
1	66	28	42%	21	32%	16	24%	1	2%	Y
2	60	23	38%	1	2%	27	45%	9	15%	Y
3	23	15	65%	3	13%	5	22%	0	0	Y
4	44	15	34%	14	32%	4	9%	11	25%	Y
5	136	40	29%	17	13%	51	38%	28	20%	Y
6	21	13	62%	6	29%	0	0	2	9%	D*
7	49	14	29%	19	39%	9	18%	7	14%	Y

8	19	8	42%	8	42%	3	16%	0	0	Y
9	94	15	16%	7	8%	32	34%	40	42%	Y
10	28	7	25%	6	21%	5	18%	10	36%	Y
11	18	9	50%	7	39%	1	6%	1	5%	Y
12	17	10	59%	1	6%	6	35%	0	0	Y
Global network	575	234	41%	85	15%	177	31%	79	13%	Y

* D: degraded bow-tie

Table 2 Node distributions in the sub-networks of the cell compartment reactions for *S. cerevisiae*

Sub-network	Total nodes	GSC		S		P		IS		Bow-tie
		nodes	percent	nodes	percent	nodes	percent	nodes	percent	
[c]	427	206	48.24%	33	7.73%	154	36.07%	34	7.96%	Y
[m]	72	35	48.61%	9	12.50%	26	36.11%	2	2.78%	Y
[x]	48	/	/	/	/	/	/	/	/	N
Global network	556	269	48.38%	39	7.01%	229	41.19%	19	3.42%	Y

Compartment Abbreviations

[c]: cytosol; [m]: mitochondrion; [x] : peroxisome

Table 3 Distribution of hub metabolites in the twelve functional modules

Module	Hub metabolite	Degree	Within-module degree	Percentage of within-module degree
1	Pyruvate	28	23	82.14%
	(S)-Lactaldehyde	10	6	60.00%

2	Acetyl-CoA Acetaldehyde Propanoyl-CoA	20 12 12	12 8 11	60.00% 66.67% 91.67%
3	Oxaloacetate	12	10	83.33%
	Citrate	11	8	72.73%
	Isocitrate	11	10	90.91%
	Glyoxylate	10	5	50.00%
	L-Aspartate	10	7	70.00%
4	L-Cysteine	10	9	90.00%
5	Glycerone phosphate (2R)-2-Hydroxy-3- (phosphonoxy)-	22 19	21 17	95.45% 89.47%
	beta-D-Fructose 6-phosphate D-Fructose 6-phosphate	16 10	10 8	62.50% 80.00%
7	alpha-D-Glucose	12	11	91.67%
	D-Galactose	11	9	81.82%
9	L-Glutamate	13	13	100.00%
10	Adenine	10	8	80.00%
12	GTP	10	10	100.00%

Additional files

Additional file 1 –Supplementary for self-similarity.pdf

Supplementary material for this paper

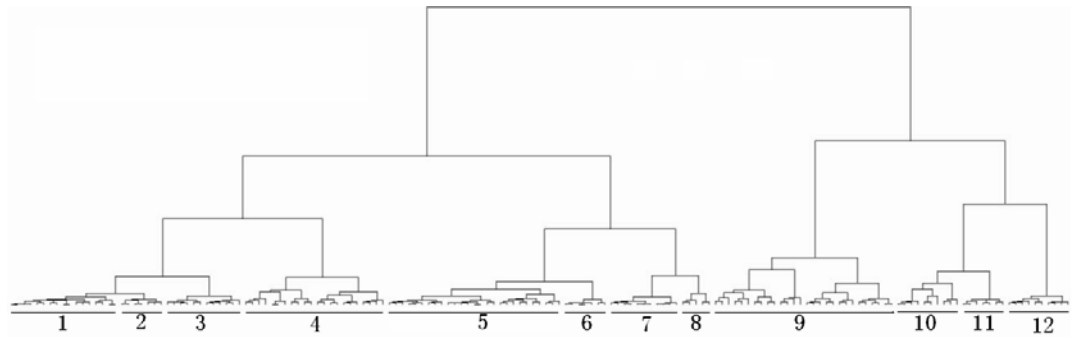


Figure1.

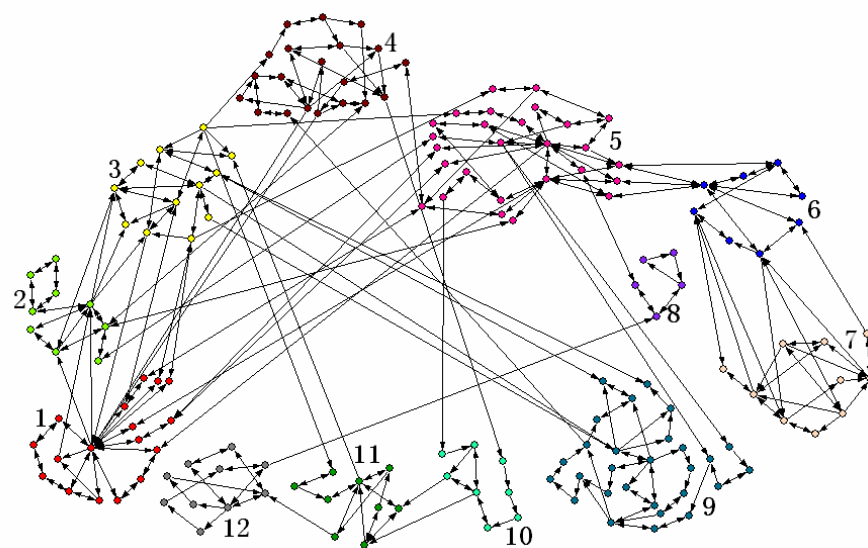


Figure 2.

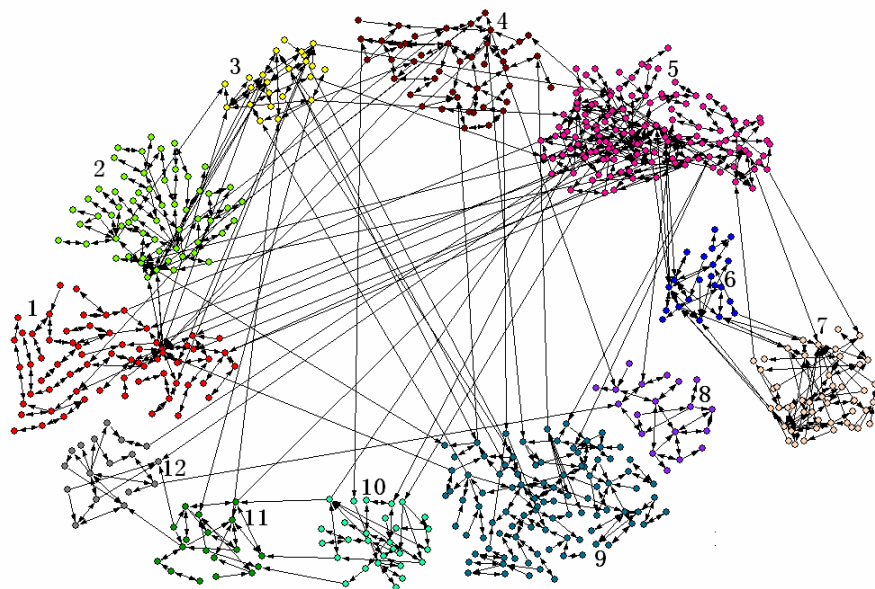


Figure 3.

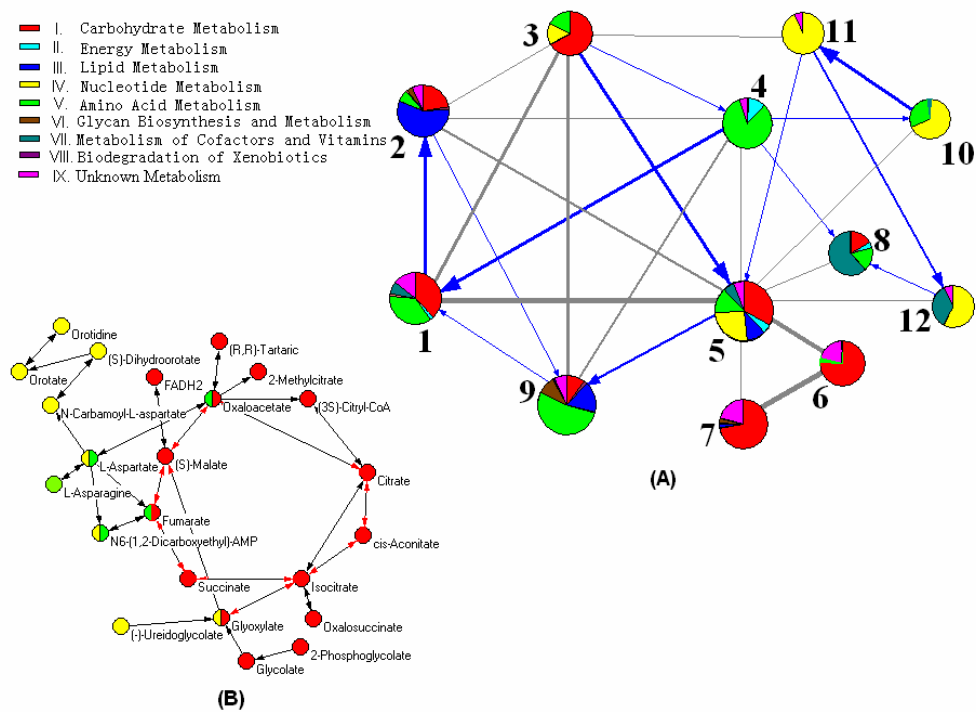


Figure 4.

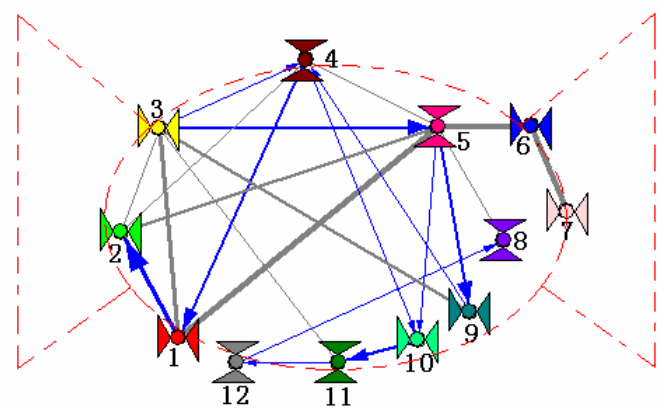


Figure 5.

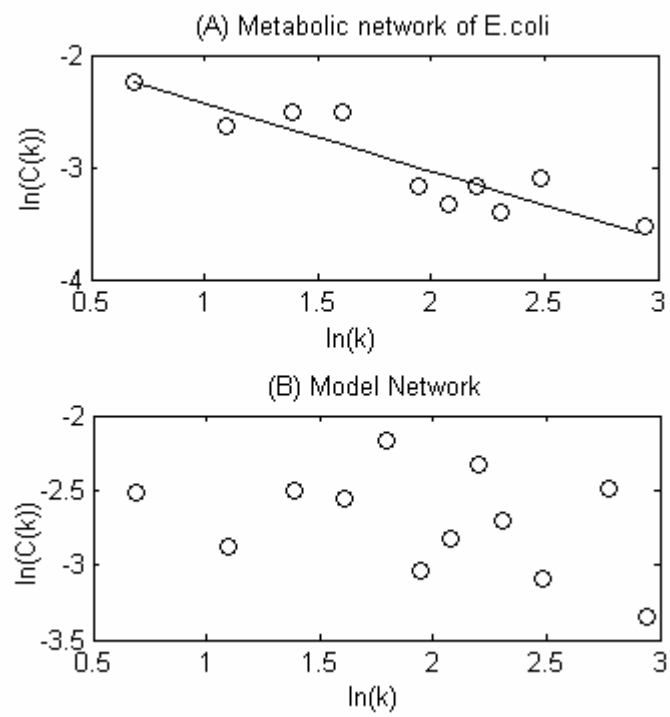


Figure 6.

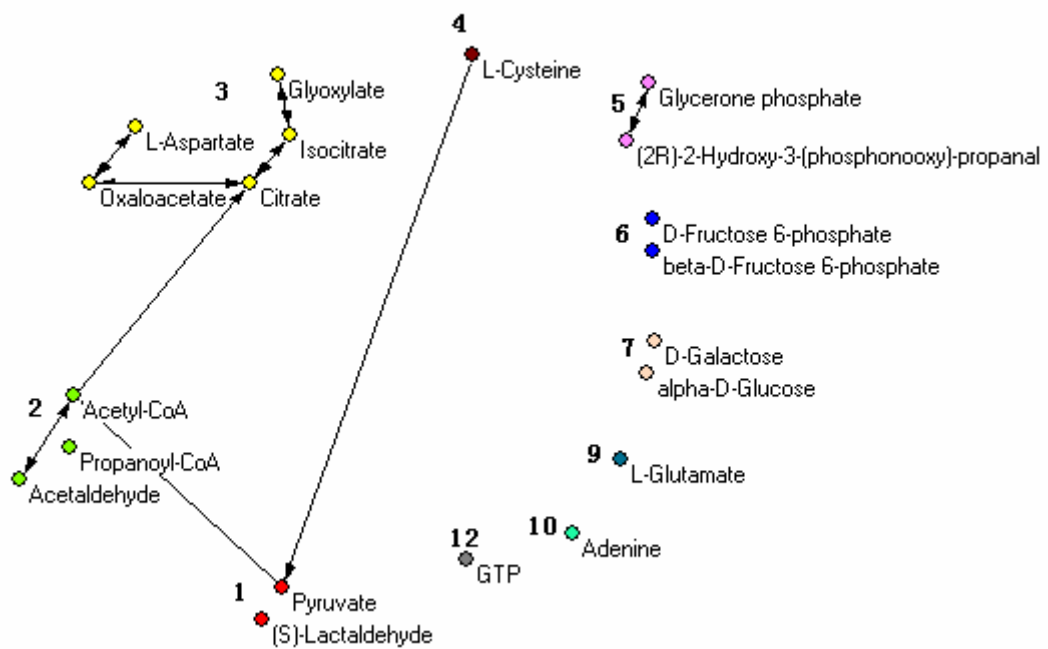


Figure 7.

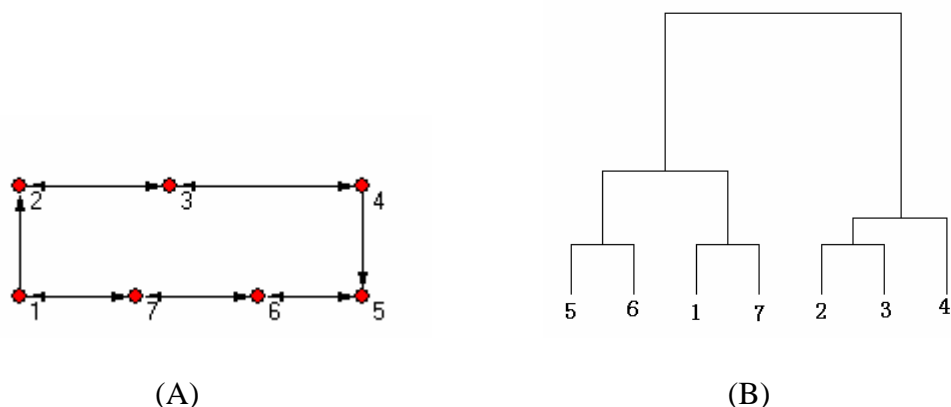


Figure 8.